Reliability analysis of deteriorating structural systems

Daniel Straub[a,*], Ronald Schneider[b], Elizabeth Bismut[a], Hyun-Joong Kim[c]

[a] *Engineering Risk Analysis Group, Technische Universität München, Germany*
[b] *Bundesanstalt für Materialforschung und -prüfung (BAM), Berlin, Germany*
[c] *COWI A/S, Lyngby, Denmark*

Abstract

Reliability analysis of deteriorating structural systems requires the solution of time-variant reliability problems. In the general case, both the capacity of and the loads on the structure vary with time. This analysis can be approached by approximation through a series of time-invariant reliability problems, which is a potentially effective strategy for cases where direct solutions of the time-variant reliability problem are challenging, e.g. for structural systems with many elements or arbitrary load processes. In this contribution, we thoroughly review the formulation of the equivalent time-invariant reliability problems and extend this approximation to structures for which inspection and monitoring data is available. Thereafter, we present methods for efficiently evaluating the reliability over time. In particular, we propose the combination of sampling-based methods with a FORM (first-order reliability method) approximation of the series system reliability problem that arises in the computation of the lifetime reliability. The framework and algorithms are demonstrated on a set of numerical examples, which include the computation of the reliability conditional on inspection data.

Keywords: reliability, deterioration, structural systems, Bayesian analysis, inspection, monitoring

1. Introduction

Deterioration can lead to decommissioning or failures of structures and infrastructures. Consequently, significant resources are spent by societies and industries to prevent or mitigate deterioration and its effects, through design measures, maintenance, inspection, monitoring, repair and retrofitting actions. To optimally plan these mitigation measures, a proper assessment of the reliability of deteriorating structures is crucial. In structural reliability, such an assessment is performed through physics-based stochastic models of the deterioration processes and the structural performance [1–3].

Computing the reliability of a deteriorating structure is a special instance of time-variant reliability analysis [4–7]. In the general case, the failure of a deteriorating system corresponds to a first-passage problem. Solutions to this problem rely on analytical solutions or numerical approximations of the outcrossing rate conditional on slowly mixing random processes and random variables [6–9]. While these methods work well for selected cases, their application to general structural systems with possibly many deteriorating elements and arbitrary load processes is challenging. That also holds for the computation of the reliability conditional on inspection and monitoring data (with the exception of some special cases).

Conveniently, for most combinations of deterioration models and structural models encountered in practice, the structural reliability can be evaluated by transforming the time-variant reliability analysis into a series of time-invariant analyses [2]. This is a common approach for application to structural systems [e.g., 10–14].

To compute the time-variant reliability of the structure based on time-invariant analyses requires the solution of a series system problem. Such an analysis can be performed at little extra computational cost when utilizing Monte Carlo simulation, but is demanding when applying advanced sampling methods. Therefore, researchers have often relied on the use of upper or lower bounds to the time-variant reliability [e.g., 10, 11, 14, 15]. Overall, efficient algorithms are desirable for the evaluation of the lifetime reliability, in particular when the structural analysis is based on numerical solutions and the number of limit state function calls should be limited. This motivates the development of efficient algorithms that can lead to results that are more exact than the bounds, but at little extra cost.

In many instances, the interest is on the reliability of a deteriorating structure conditional on inspection and monitoring data [e.g., 14, 16]. To the best of our knowledge, no rigorous treatment of the conditional lifetime reliability of structural systems and its computation based on the time-invariant formulation can be found in the literature. In particular, as we show in this paper, for computing the

*Corresponding author
Email address: straub@tum.de (Daniel Straub)

reliability at time t conditional on inspection or monitoring data up to time t_Z, it generally is not sufficient to evaluate the conditional reliability only for time intervals after t_Z. Instead, it is necessary to evaluate the conditional reliability for all time intervals.

The paper starts out by revisiting the basic definitions of reliability in deteriorating structural systems and the different cases in which the reliability can be evaluated or approximated through time-invariant reliability analyses. We describe and demonstrate the necessary computations when considering reliability updating with inspection and monitoring results.

We then propose efficient strategies for the computation of the structures lifetime reliabilities through analytical approximations (FORM), sampling-based approaches and combinations thereof. We present computational strategies for improved efficiency of the time-invariant reliability evaluations, and we propose an approach for estimating the time-variant reliability without additional limit state function calls. The principles and computational strategies are investigated and demonstrated on a set of four numerical examples.

2. Reliability of deteriorating structural systems

2.1. General

At time t, a structure can – at least conceptually – be characterized by its capacity $R(t)$ and the demand on the structure[1] $S(t)$. The corresponding safety margin is [3]

$$M(t) = R(t) - S(t). \tag{1}$$

More generally, the system can be modeled by a limit state function[2] $g(\mathbf{X}, t)$. Therein, $\mathbf{X}$ is the vector of input random variables [1, 2, 17]. By definition, a negative value of the limit state function corresponds to a failure of the system. The safety margin $M(t)$ is an instance of the limit state function with input random variables $\mathbf{X} = [R(t); S(t)]$. One can define a point-in-time failure event[3] as

$$F^*(t) = \{R(t) \leq S(t)\}, \tag{2}$$

or, more generally, as

$$F^*(t) = \{g(\mathbf{X}, t) \leq 0\}. \tag{3}$$

Computation of the corresponding probability $\Pr[F^*(t)]$ is typically straightforward, as discussed in Section 3.2; consequently, this quantity is frequently used to assess the reliability of deteriorating structures [13, 14, 18–20]. However, for decision making purposes, e.g. in design or integrity management, this quantity can be misleading, because it does not capture the history leading up to time t. In particular, it neglects that the system may already have failed previously and the model $R(t)$ or $g(\mathbf{X}, t)$ has no actual meaning in this case.

To describe the reliability of the structure at time t, one must therefore consider the random processes $\{R(\tau)\}_{\tau\in[0,t]}$ and $\{S(\tau)\}_{\tau\in[0,t]}$ and compute the accumulated failure event, which defines the event of failure at any time up to t:

$$F(t) = \{\exists\tau \in [0, t], R(\tau) \leq S(\tau)\}, \tag{4}$$

or

$$F(t) = \left\{ \left[\min_{\tau\in[0,t]} g(\mathbf{X}, \tau) \right] \leq 0 \right\}. \tag{5}$$

Utilizing the more general definition of Eq. 5, the probability of a failure up to time t is

$$\Pr[F(t)] = \Pr\left\{ \left[\min_{\tau\in[0,t]} g(\mathbf{X}, \tau) \right] \leq 0 \right\}. \tag{6}$$

All quantities that are commonly used to describe the lifetime reliability can be computed from $\Pr[F(t)]$ [21]. These include the cumulative distribution function (CDF) of the structure's lifetime T,

$$F_T(t) = \Pr(T \leq t) = \Pr[F(t)], \tag{7}$$

and the corresponding probability density[4]

$$f_T(t) = \frac{d}{dt} F_T(t). \tag{8}$$

The reliability of the structure is

$$Rel(t) = 1 - \Pr[F(t)]. \tag{9}$$

The hazard function is

$$h(t) = \frac{f_T(t)}{Rel(t)}. \tag{10}$$

$h(t)$ describes the failure rate of the structure conditional on it having survived up to time t.

The function $\Pr[F(t)]$ and the derived quantities summarized above describe the reliability of a single structural system. When the system fails, it might be systematically replaced. Such a process can be described by renewal theory [23, 24], which enables calculation of the cost and risk of the system considering replacement. Such studies have been performed, e.g. for optimizing risk acceptance criteria [25, 26]. The focus of the current paper is on individual

[1] Depending on the formulation, $S(t)$ is either the load or the load effect.

[2] Often, the system is characterized by multiple limit state functions $g_i(\mathbf{X}, t)$ representing different system failure mechanisms. These can always be combined to a single limit state function by $g(\mathbf{X}, t) = \min\{g_1(\mathbf{X}, t), g_2(\mathbf{X}, t), \dots\}$, even if this may not be optimal for computational purposes.

[3] $F^*(t)$ is also termed instantaneous failure event and the corresponding $\Pr[F^*(t)]$ is termed instantaneous failure probability in the literature [2, 3].

[4] The probability density $f_T(t)$ is sometimes referred to as the unconditional failure rate [2, 22]. We avoid this name, because in the system reliability literature the term failure rate is used exclusively to denote the conditional rate, Eq. 10 [21].

structural systems with high reliability, without considering their replacement. However, the lifetime distribution of the structure $F_T(t) = \Pr[F(t)]$, which is the result of the models and algorithms presented in the following, can be the basis for a renewal process analysis.

In summary, the reliability performance of a deteriorating structure without maintenance and repair actions is fully described by $\Pr[F(t)]$. In the general case, computing $\Pr[F(t)]$ requires the solution of a first-passage problem. However, most deteriorating structures can be represented by stochastic deterioration models that correspond to classes (a) and (b) in Figure 1. For these classes, the time-variant reliability problem can be transformed into a series of time-invariant reliability problems. These are presented in Sections 2.2 and 2.3. The main focus of this paper lies on the deterioration model class (b). For completeness, Figure 1c represents problems that cannot be adequately represented by classes (a) or (b) and require the solution of the general first-passage problem. An example is low-cycle fatigue, in which the damage propagates only when large load events occur, as illustrated in Figure 1c.

In Section 2.4, we consider the computation of $\Pr[F(t)]$ conditional on inspection and monitoring data and in Section 2.5 conditional on repair actions.

2.2. Stochastic deterioration models resulting in monotonically decreasing limit state functions

The first class of stochastic deterioration models for structures are those in which the limit state function $g(\mathbf{X}, t)$ describing failure is monotonically decreasing with time t for any value of $\mathbf{X}$ (Figure 1a). Deterioration is described by a function $h_d(\mathbf{X}, t)$ and failure occurs when deterioration exceeds some limit D_{cr} (which might also be a random variable and thus part of $\mathbf{X}$). The corresponding generic limit state function is

$$g(\mathbf{X}, t) = D_{cr} - h_d(\mathbf{X}, t). \tag{11}$$

For example, fatigue modeled with the Palmgren-Miner damage accumulation rule and SN curves falls into this category [e.g., 1, 27]. Other examples are deterioration models based on gamma processes, where failure occurs when the resistance falls below a (possibly probabilistic) level [28, 29].

A monotonically decreasing $g(\mathbf{X}, t)$ signifies that $\min_{\tau \in [0,t]} g(\mathbf{X}, \tau) = g(\mathbf{X}, t)$. Inserting this equality into Eq. 5 results in

$$F(t) = \{g(\mathbf{X}, t) \leq 0\} = F^*(t). \tag{12}$$

Hence the failure event $F(t)$ is equivalent to the point-in-time failure event $F^*(t)$, because the safety margin will be negative at time t if it is negative at any time prior to t. As a consequence, it is

$$\begin{aligned} \Pr\left[F(t)\right] &= \Pr\left[F^*(t)\right] \\ &= \Pr\left[g(\mathbf{X}, t) \leq 0\right]. \end{aligned} \tag{13}$$

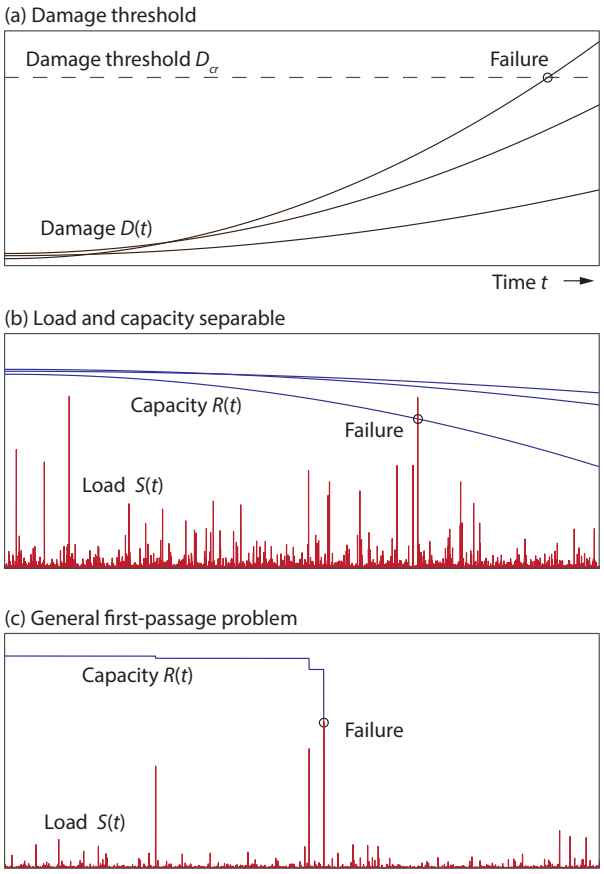

Figure 1: Classes of stochastic deterioration models. Class (a) are problems, in which the system is described by a non-decreasing damage function and failure occurs when the damage exceeds a threshold. Class (b), which is the main focus of this paper, are problems in which the (deteriorating) capacity $\{R(t)\}$ can be modeled independently of the load process $\{S(t)\}$. Class (c), here represented by an example of low-cycle fatigue, are problems in which the capacity and load processes cannot be modeled independently.

Because the computation of $\Pr\left[F^*(t)\right]$ is typically straightforward (see Section 3.2), the computation of the lifetime reliability can be performed without difficulties for this class of deterioration models.

Note that the requirement of a monotonically decreasing $g(\mathbf{X}, t)$ precludes the effect of maintenance and repair actions, which are considered in Section 2.5.

2.3. Deteriorating structures with separable demand and capacity variables

A second common class of stochastic deterioration models is illustrated in Figure 1b. These are models in which the random variables or processes $\mathbf{X}$ can be separated into a group $\mathbf{X}_S$ determining demands and a group $\mathbf{X}_R$ determining capacity.

In the simplest case, failure of the structure can be described by a safety margin of the form of Eq. 1, $M(t) = R(\mathbf{X}_R, t) - S(t)$. This is the case when the load or load effect at time t can be summarized by a scalar random vari-

able[5] $S(t)$ and the capacity of the structure with respect to that load or load effect can be determined as $R(\mathbf{X}_R, t)$. The capacity $R(\mathbf{X}_R, t)$ includes the deterioration process and is a monotonically decreasing function of t.

Conveniently, time is discretized in intervals $j = 1, \ldots, m$, such that the jth interval corresponds to $t \in (t_{j-1}, t_j]$. A common choice is yearly intervals, but finer discretization can be desirable if the service life is short or if inspection or maintenance intervals are shorter than one year.

By analogy with the point-in-time failure event $F^*(t)$, we define the *interval failure* event F_j^* as the event of a failure in $(t_{j-1}, t_j]$, neglecting the occurrence of previous failure events:

$$F_j^* = \left\{ \left[\min_{\tau \in (t_{j-1}, t_j]} g(\mathbf{X}, \tau) \right] \leq 0 \right\}. \tag{14}$$

Exact computation of the corresponding probability $\Pr(F_j^*)$ is challenging, but if the load can be summarized by a scalar variable, a good approximation is

$$\Pr(F_j^*) \approx \Pr\left[R(\mathbf{X}_R, t_j) \leq S_{max,j}\right], \tag{15}$$

wherein $S_{max,j}$ is

$$S_{max,j} = \max_{t \in (t_{j-1}, t_j]} S(t), \tag{16}$$

the maximum demand in time interval j. For example, $S_{max,j}$ can be the load effect of the annual maximum wind load. The statistics of $S(t)$ are obtained by an extreme value analysis. $\Pr\left[R(\mathbf{X}_R, t_j) \leq S_{max,j}\right]$ in Eq. 15 can be evaluated by a time-invariant reliability analysis. This is the strong benefit of this formulation.

Note that the approximation made in Eq. 15 is strictly conservative, because the maximum demand in the time interval, $S_{max,j}$, is compared with the minimum capacity in the interval, $R(\mathbf{X}_R, t_j)$. The error is bounded by $\Pr\left[R(\mathbf{X}_R, t_j) \leq S_{max,j}\right] - \Pr\left[R(\mathbf{X}_R, t_{j-1}) \leq S_{max,j}\right]$, which typically is a small number[6]. The error can be controlled by the choice of the time interval durations.

Challenges to this reliability analysis may arise when $R(t)$ and $S(t)$ cannot be considered as statistically independent. Note that in many real life applications, $R(t)$ and $S(t)$ are not strictly independent. Nevertheless, the assumption of independence is often justified. As an example, fatigue deterioration is determined by cyclic loading, which is related to the extreme loads $S(t)$. For high-cycle fatigue, however, only a small part of the deterioration damage is associated to those extreme events, and independence among $R(t)$ and $S(t)$ is a justified assumption (and a common one in the literature [1]). The same may not hold for low-cycle fatigue (which is illustrated in Figure 1c), as discussed in [6].

In many structures, it is not possible to summarize the loads on the system in a single scalar variable $S(t)$. Instead, the demand is summarized by a vector[7] $\mathbf{S}(t)$; e.g., the demand on an offshore structure at time t is the joint effect of wind speed, wave height and current velocity at t. Therefore, a limit state function $g[\mathbf{X}_R, \mathbf{S}(t), t]$ has to be considered.

It is conducive to split the load vector into time-variant loads $\mathbf{S}_{\mathrm{tv}}(t)$ and time-invariant loads $\mathbf{S}_{\mathrm{ti}}$, which are constant over the entire service life of the structure[8]. If multiple of the loads are time-variant, the evaluation of $\Pr(F_i^*)$ must consider the load-combination problem. The exact solution of this problem requires the solution of an outcrossing problem, which can itself only be solved approximately in the general case. Alternatively, approximate formulations involving only time-invariant random variables are available [2, 30–32]. If one of the time-varying loads is dominating, the load-combination problem can be reduced to applying the extreme value distribution of the dominating load and the conditional distributions of the remaining time-variant loads, summarized in the load vector $\mathbf{S}_{max,j}$ for the time interval j. The interval probability of failure can then be evaluated as

$$\Pr(F_j^*) \approx \Pr\left[g\left(\mathbf{X}_R, \mathbf{S}_{max,j}, \mathbf{S}_{\mathrm{ti}}, t_j\right) \leq 0\right]. \tag{17}$$

Here the capacity during the time interval j is approximated with the capacity at time t_j, in analogy to the approximation of Eq. 15. When only one time-variant load process is present, $\mathbf{S}_{max,j}$ in Eq. 17 is replaced by $S_{max,j}$.

To evaluate $\Pr[F(t_i)]$, we note that the event of a structural failure up to time t_i is the union of the interval failure events $\Pr(F_j^*)$ leading up to t_i:

$$\Pr\left[F(t_i)\right] = \Pr\left(F_1^* \cup F_2^* \cup \cdots \cup F_i^*\right). \tag{18}$$

In the general case, the events F_j^* are dependent, hence knowledge of the $\Pr(F_j^*)$ is not sufficient to compute $\Pr[F(t_i)]$. However, bounds can be found as [33]:

$$\max_{j \in [1,\ldots,i]} \Pr(F_j^*) \leq \Pr\left[F(t_i)\right] \leq \sum_{j=1}^{i} \Pr(F_j^*). \tag{19}$$

If the maximum demands $\mathbf{S}_{max,j}$ are mutually independent, or if their dependence is positive, the statistical dependence among the $\Pr(F_j^*)$ will be non-negative[9].

[5] $S(t)$ can also be a function of other random variables $\mathbf{X}_S$, e.g. when the distribution of $S(t)$ is subject to parameter uncertainty or when $S(t)$ is the load effect that depends on properties of the structure. This dependence is omitted here for readability.

[6] I.e., the true interval failure probability for interval j must lie between the estimates for intervals $j-1$ and j. Therefore, the maximum error that can result from this approximation corresponds to a shift of the estimated $\Pr(F_j^*)$ by one year. In most cases, the actual error is significantly smaller than that.

[7] This vector can be dependent on other variables $\mathbf{X}_S$.

[8] With some modifications, the methodology presented in this paper is also applicable to the case where the loads are constant only over a fraction of the service life.

[9] Non-negative dependence implies that $\Pr(F_{j_1}^* | F_{j_2}^*) \geq \Pr(F_{j_1}^*)$ for any j_1 and j_2. Note that the resistances $R(\mathbf{X}_R, t_j)$ will be positively correlated among different t_j.

Hence a narrower upper bound can be found based on independent interval failure events:

$$\max_{j\in[1,\dots,i]} \Pr(F_j^*) \leq \Pr\left[F(t_i)\right] \leq 1 - \prod_{j=1}^{i} \left[1 - \Pr(F_j^*)\right]. \quad (20)$$

If the reliability is dominated by uncertainty on the demands $\mathbf{S}_{max,j}$, $\Pr[F(t_i)]$ will be closer to the upper bound of Eq. 20. Conversely, if the reliability is dominated by uncertainty on $R(t)$ or $\mathbf{S}_{\text{ti}}$, $\Pr[F(t_i)]$ will be closer to the lower bound. The upper bound in Eq. 20 has been used in the literature as an approximation of $\Pr[F(t_i)]$, e.g. in [10, 12, 34]

Exact computation of $\Pr\left[F(t_i)\right] = \Pr\left[F_1^* \cup F_2^* \cup \dots \cup F_i^*\right]$ involves the solution of a system reliability problem. While such a problem can be solved, the direct evaluation of the probability of the union is associated with increased computational cost and is often less accurate[10]. Therefore, we propose a novel approach to evaluating $\Pr[F(t_i)]$ in Section 3.3.

Once the probabilities $\Pr[F(t_i)]$ are computed for times $t_1, t_2, \dots, t_i$, the full function $F_T(t) = \Pr[F(t)]$ can be approximated by interpolation. The reliability and the hazard function (failure rate) then follow from $F_T(t)$.

2.4. Deteriorating structures with inspection and monitoring data

On many structures, inspection and monitoring are employed to reduce the uncertainty on the condition $R(t)$ or the loading $S(t)$. The information provided by inspection or monitoring data can be included through Bayesian updating of the failure probabilities [35–37]. In the context of structural reliability, the data available up to time t can be described by an event $Z(t)$, and the updated probability is $\Pr\left[F(t)|Z(t)\right]$ [37, 38].

In computing $\Pr\left[F(t)|Z(t)\right]$, it should be kept in mind that $Z(t)$ does not alter the "inherent" reliability of the structure, since the information has no effect on the actual physical system[11]. $Z(t)$ does however alter one's estimate of the reliability. Once the information $Z(t)$ is obtained, the probability distribution of the random variables $\mathbf{X}$ is updated from $f_{\mathbf{X}}$ to $f_{\mathbf{X}|Z(t)}$, and as a result the reliability is updated as well [39]. The complete theory presented thus far holds also for the conditional distributions and probabilities.

For the stochastic deterioration model class (b), the probability of failure at time t_i conditional on data up to time t_Z is found by conditioning Eq. 18 on $Z(t_Z)$:

$$\Pr\left[F(t_i)|Z(t_Z)\right] = \Pr\left[F_1^* \cup F_2^* \cup \dots \cup F_i^* |\, Z(t_Z)\right]. \quad (21)$$

This result has an important implication: For computing the reliability at time t_i, it is not sufficient to consider only the interval failure events from time t_Z on, but all intervals starting at $j = 1$ must be considered. Therefore, whenever new data arise, the entire history $F_1^* - F_i^*$ must be reconsidered conditional on the entire data.

This implication may seem counterintuitive. Reliability estimates conditional on data are typically shown as $\Pr\left[F(t_i)|Z(t_i)\right]$, i.e. the probability of failure at time t_i is presented conditional on all data available up to time t_i. This is known as *filtering*. However, data obtained at a time t_Z nevertheless influence the reliability estimates for times $t < t_Z$, in a process known as *smoothing* [40]: The data allow updating of the distribution of $\mathbf{X}$, which includes $\mathbf{X}_R$, that affects the probability of all F_j^*, independent of whether data has been obtained prior to or after t_j. The difference between filtering and smoothing is illustrated further below in Figure 11.

If data is collected at t_Z, the structure must have survived up to this point and one can condition on this survival event, by analogy with the computation of the hazard function. Does that imply that the interval failure events prior to t_Z can be neglected in this case, because they are known not to have occurred? Unfortunately no. In the general case, the survival of these events contains information, and that information is affected by $Z(t_Z)$. Formally, for any $t_i > t_Z$ it is

$$\begin{aligned} &\Pr\left[F(t_i)\,\middle|\, Z(t_Z) \cap \overline{F(t_Z)}\right] \\ &= \frac{\Pr\left[F(t_i) \cap \overline{F(t_Z)}\,\middle|\, Z(t_Z)\right]}{\Pr\left[\overline{F(t_Z)}\,\middle|\, Z(t_Z)\right]} \\ &= \frac{\Pr\left[F(t_i)|\, Z(t_Z)\right] - \Pr\left[F(t_Z)|\, Z(t_Z)\right]}{1 - \Pr\left[F(t_Z)|\, Z(t_Z)\right]}. \end{aligned} \quad (22)$$

Both probabilities on the right hand side of Eq. 22 must be evaluated following Eq. 21.

Instead of evaluating Eq. 22, one would typically compute the more general hazard function (Eq. 10) that conditions on survival at any year, not only on survival at time t_Z. To evaluate the hazard function conditional on the data, one has to first evaluate $\Pr\left[F(t_i)|Z(t_Z)\right]$. The hazard function given $Z(t_Z)$ is then obtained by replacing $\Pr\left[F(t_i)\right]$ in Eqs. 8-10 with $\Pr\left[F(t_i)|Z(t_Z)\right]$. This is illustrated in Section 4.2.1.

In summary, for the stochastic deterioration model class (b), computation of the reliability conditional on data requires the evaluation of the entire history conditional on the data, irrespective of the time at which the data is obtained. This leads to an increased computational effort, which seems not to have been recognized previously.

Note that in case of the stochastic deterioration model class (a), the above is not relevant. Because $\Pr\left[F(t)|Z(t_Z)\right] = \Pr\left[F^*(t)|Z(t_Z)\right]$, it is sufficient to compute the latter.

2.5. Deteriorating structures with maintenance and repair actions

Maintenance and repair actions lead to changes in the distribution of $R(t)$. In many instances, the condition of

[10] The exception being an evaluation with crude Monte Carlo simulation, as discussed in Section 3.1.

[11] The actions taken based on the information, such as repair or retrofitting actions, do alter the system (Section 2.5).

the structure after a repair action at time t_{rep} can be considered as statistically independent of the condition prior to the repair. If the loading is also independent before and after t_{rep}, then the reliability of the structure can be computed from t_{rep} on, without consideration of the events prior to t_{rep}. If the variables are dependent, then it is necessary to compute the full history, wherein the repair is modeled by adding new random variables or processes describing $R(t)$ for times $t \geq t_{rep}$.

3. Efficient computational strategies for computing the reliability of deteriorating structures

In this section, we present and propose methods for effectively computing the failure probability $\Pr[F(t)]$, either directly or through the interval failure probability $\Pr(F_i^*)$.

3.1. Monte Carlo simulation

Monte Carlo simulation (MCS) is the simplest and most robust solution strategy to computing the reliability of deteriorating structures. Accounting for dependence among the failure events in multiple time periods is straightforward with MCS. The disadvantage of MCS is its inefficiency, in particular when computing small probabilities. This makes MCS infeasible for problems that involve computationally costly limit states, and for most problems that require the computation of the reliability conditional on inspection results. However, whenever MCS is computationally feasible, it should be the method of choice.

MCS proceeds by generating samples $\mathbf{x}^{(k)}, k = 1, \ldots, n_s$, of $\mathbf{X}$. For stochastic deterioration model class (b), the probability of failure is estimated based on Section 2.3 as

$$\Pr\left[F\left(t_i\right)\right] \approx \frac{1}{n_s} \sum_{k=1}^{n_s} \mathbb{I}\left\{ \left[\min_{j=1:i} g\left(\mathbf{x}_R^{(k)}, \mathbf{s}_{max,j}^{(k)}, \mathbf{s}_{\mathrm{ti}}^{(k)}, t_j \right) \right] \leq 0 \right\}. \tag{23}$$

$\mathbb{I}[]$ is the indicator function, which takes value 1 if its argument holds and 0 otherwise.

Note that the evaluations of the limit state functions $g\left(\mathbf{x}_R^{(k)}, \mathbf{s}_{max,j}^{(k)}, \mathbf{s}_{\mathrm{ti}}^{(k)}, t_j\right)$ can be reused when evaluating $\Pr\left[F\left(t_i\right)\right]$ for different i. The Monte Carlo method is very robust in the sense that the accuracy of the probability of failure estimate depends only on the probability of failure itself. In both cases above, the coefficient of variation (c.o.v.) of the MCS estimate is

$$\delta_{MCS} = \frac{\sqrt{p - p^2}}{p\sqrt{n_s}} \approx \frac{1}{\sqrt{p\, n_s}}, \tag{24}$$

wherein p is either $\Pr\left[F\left(t\right)\right]$ or $\Pr\left[F\left(t_i\right)\right]$.

It follows from Eq. 24 that to achieve a c.o.v. of the estimate of 10%, the required number of samples (and hence evaluation of the model g) is $n_s = \frac{100}{\Pr[F(t_i)]}$. For a $\Pr\left[F\left(t_i\right)\right]$ in the order of 10^{-6}, around 10^8 model evaluations are required. This is only feasible for simple analytical models (which could be surrogate models).

When computing the reliability conditional on inspection or monitoring data, one can estimate $\Pr[F(t_i)|Z(t_Z)]$ with Eq. 23 by generating samples $\mathbf{x}^{(k)}$ that follow the conditional distribution $f_{\mathbf{X}|Z(t)}$. This can be achieved by any Bayesian algorithm that generates posterior samples, including MCMC methods [e.g., 41] and the BUS approach [37, 38]. Note that the computational demands by an MCS analysis might increase by additional orders of magnitude in the conditional case if updating the distribution of $\mathbf{X}$ requires evaluations of the deterioration or structural model [39].

3.2. Efficient computation of $\Pr[F^*(t)]$ *or* $\Pr[F_i^*]$

Computation of $\Pr[F^*(t)] = \Pr[F(t)]$ for the stochastic deterioration model class (a) or $\Pr[F_i^*]$ for class (b) requires the solution of time-invariant reliability problems. A large number of methods exist for this purpose, which include approximation methods, in particular FORM and SORM (first-/second-order reliability method), and sampling-based methods. Here, we exemplary consider FORM and subset simulation (SuS), but note that the strategies presented here can be extended to other methods. For example, sequential importance sampling [42], line sampling [43–45] or other importance sampling techniques [e.g., 46, 47] might be considered instead of SuS. All these structural reliability methods are optimized for computing $\Pr[g_j(\mathbf{X}) \leq 0]$. Here, $g_j(\mathbf{X})$ is utilized as short notation for the limit state function $g\left(\mathbf{X}_R, \mathbf{S}_{max,j}, \mathbf{S}_{\mathrm{ti}}, t_j\right)$ in Eq. 17, whereby $\mathbf{X} = [\mathbf{X}_R; \mathbf{S}_{max,i}; \mathbf{S}_{\mathrm{ti}}]$.

3.2.1. FORM

FORM is based on a transformation of the random variables $\mathbf{X}$ entering the limit state function to corresponding uncorrelated standard normal random variables $\mathbf{U} = T(\mathbf{X})$ [30]. This is achieved by means of the Rosenblatt transformation [48] or the Nataf transformation [49], see also [17]. The limit state function is then expressed in terms of $\mathbf{U}$:

$$G_j(\mathbf{u}) = g_j\left[T^{-1}(\mathbf{u})\right], \tag{25}$$

wherein T^{-1} denotes the inverse transform.

FORM linearizes the limit state function in standard normal space around the most likely failure point (MLFP) $\mathbf{u}_j^*$, also known as design point. It is defined as

$$\begin{aligned} &\mathbf{u}_j^* = \arg\min \|\mathbf{u}\| \\ &\text{s.t. } G_j(\mathbf{u}) \leq 0. \end{aligned} \tag{26}$$

where $\|\,.\,\|$ denotes the Euclidian norm.

$\beta_j = \|\mathbf{u}_j^*\|$ is the reliability index. Because of the properties of the standard normal space, the probability of failure associated with the linearized limit state function is a function solely of β_j. This is the FORM approximation of $\Pr(F_j^*)$:

$$\Pr(F_j^*) \approx \Phi(-\beta_j), \tag{27}$$

with Φ being the standard normal CDF.

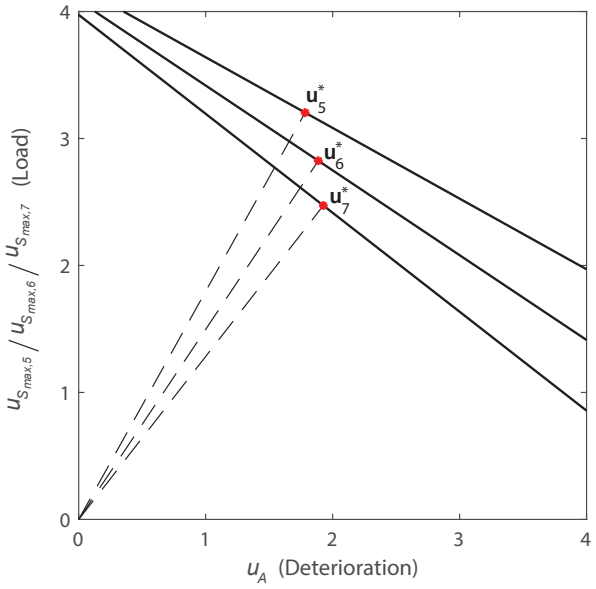

Figure 2: MLFPs and limit state surfaces associated with interval failure events in three subsequent years. Note the dimension of the ordinate is changing with the considered time interval i. MLFPs and the limit state surfaces are plotted for year 5 to 7, for ratio=0.5. MLFPs are $\mathbf{u}_5^* = [1.78; 3.20]$, $\mathbf{u}_6^* = [1.89; 2.82]$ and $\mathbf{u}_7^* = [1.93; 2.47]$. These are the results of Section 4.2 with $ratio = 0.5$.

FORM is typically efficient and accurate for problems with limited number of random variables $\mathbf{X}$ [44]. The computationally expensive part of the analysis is the solution of the minimization problem, Eq. 26.

In cases where the evaluation of the limit state function g_j is expensive, one can further reduce the computation cost by exploiting the fact that the solution of Eq. 26 is similar for subsequent time intervals. Thereby, the solution $\mathbf{u}_{j-1}^*$ can be taken as the starting point when solving Eq. 26.

The input random variables describing time-variant loads $\mathbf{S}_{max,j}$ vary among time intervals j. When the $\mathbf{S}_{max,j}$ are iid (independent, identically distributed) for different j, the MLFP found for time interval j is nevertheless a close starting point for $j+1$ when replacing $u_{S_{max,j}}$ with $u_{S_{max,j+1}}$, as illustrated in Figure 2.

3.2.2. Subset simulation

Subset simulation (SuS) [50] is based on formulating the sought probability $\Pr(F_j^*) = \Pr[g_j(\mathbf{X}) \leq 0]$ through a sequence of conditional probabilities

$$\Pr[g_j(\mathbf{X}) \leq 0] = \prod_{k=1}^{M} \Pr[g_j(\mathbf{X}) \leq h_k | g_j(\mathbf{X}) \leq h_{k-1}]. \quad (28)$$

M is the number of subsets and h_k are the intermediate thresholds, with $\infty = h_0 > h_1 > \cdots > h_{M-1} > h_M = 0$. In this way, $\{g_j(\mathbf{X}) \leq h_k\}$ is a subset of $\{g_j(\mathbf{X}) \leq h_{k-1}\}$, which ensures the validity of Eq. 28.

The intermediate thresholds h_k are selected such that the conditional probabilities in Eq. 28 are sufficiently large, typically around 0.1. Hence standard Monte Carlo can be applied to compute these conditional probabilities, whereby samples of $\mathbf{X}$ are generated with Markov Chain Monte Carlo (MCMC). For details on the implementation we refer to [50, 51].

SuS can handle high-dimensional problems, i.e. many random variables in $\mathbf{X}$. It does however require a significantly higher number of limit state function calls than FORM, commonly in the order of $10^3 - 10^4$. Separately solving $\Pr(F_j^*) = \Pr[g_j(\mathbf{X}) \leq 0]$ with SuS for different j is thus inefficient. Instead, one should exploit that the capacity is monotonically decreasing under deterioration, which implies that $g(\mathbf{X}_R, \mathbf{S}_{max}, \mathbf{S}_{\text{ti}}, t_j) \geq g(\mathbf{X}_R, \mathbf{S}_{max}, \mathbf{S}_{\text{ti}}, t_{j+1})$. The failure event corresponding to the first limit state function is therefore a subset of the failure event corresponding to the second. Note that here we have omitted the index j for the load random variables $\mathbf{S}_{max}$, implying that the same maximum load applies in all time intervals. In reality those are different, and failure in time interval j is not a subset of failure in $j+1$, as discussed in Section 2.3. However, as long as all $\mathbf{S}_{max,j}$ are iid, they can all be replaced by the same $\mathbf{S}_{max}$ and one can consider F_j^* to be a subset of F_{j+1}^* for the purpose of computing the individual $\Pr(F_j^*)$.

This gives rise to the following efficient computational procedure: The interval failure probability $\Pr(F_j^*)$ of the last interval i is computed first, with SuS following Eq. 28. The probability of the preceding time interval $j-1$ is then computed as

$$\Pr(F_{j-1}^*) = \Pr(F_{j-1}^* | F_j^*) \Pr(F_j^*). \quad (29)$$

$\Pr(F_{j-1}^* | F_j^*)$ is estimated by generating samples of $\mathbf{X}$ conditional on F_j^* via MCMC[12]. If $\Pr(F_{j-1}^* | F_j^*)$ is significantly larger than the selected conditional probability of intermediate thresholds (commonly 0.1), the same samples might be used to compute also $\Pr(F_{j-2}^* | F_j^*)$, $\Pr(F_{j-3}^* | F_j^*)$ and so on, until the conditional probability is smaller than 0.1. A new subset level is then introduced at the last interval failure event for which $\Pr(F_{j-k}^* | F_j^*) \geq 0.1$.

In case that $\Pr(F_{j-1}^* | F_j^*) \leq 0.1$, additional subset levels can be introduced, as in standard SuS.

The sequential computation with SuS is illustrated in Figure 3. The efficiency of this sequential approach to computation is presented and investigated in more details in [54].

3.3. Efficient computation of $\Pr[F(t_i)] = \Pr(F_1^* \cup F_2^* \cup \cdots \cup F_i^*)$

For the stochastic deterioration model class (b), the bounds on the probability of failure $\Pr[F(t_i)]$ are readily determined from the interval failure probabilities $\Pr(F_i^*)$ according to Eq. 20. However, these bounds are often wide and a more accurate estimate of $\Pr[F(t_i)]$ is desirable.

[12] This choice of the intermediate threshold also ensures that the resulting estimate is unbiased, because the threshold is not selected adaptively (see Section 9.6 of [52], also [53]).

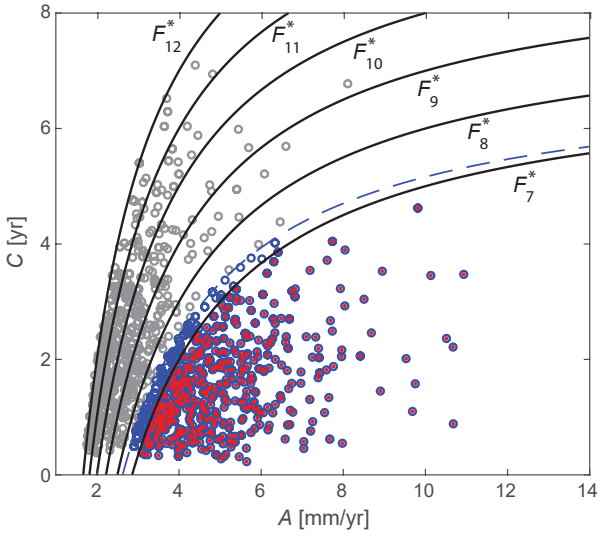

Figure 3: Samples of multiple subset simulation steps. The grey samples are conditional on F_{12}^* and are used to evaluate the probabilities of F_{11}^* to F_8^*. The dashed line represents a new subset level that is introduced to compute $\Pr(F_7^*)$ and beyond (colored samples). These are results of Section 4.1.

Such an estimate is readily available through a FORM system analysis (Section 3.3.1). We propose to extend the FORM solution to cases where the $\Pr(F_i^*)$ are computed through sampling-based methods (Section 3.3.2). Finally, in Section 3.3.3 we discuss the computation of $\Pr[F(t_i)]$ when the structural system performance is described by the conditional probability of structural failure given the condition of the structure, $\Pr(F_i^*|\mathbf{X}_R = \mathbf{x}_R)$.

3.3.1. FORM

FORM facilitates an efficient computation of $\Pr(F_1^* \cup F_2^* \cup \cdots \cup F_i^*)$, since it requires as an input only the FORM reliability indexes β_j^* associated with the individual $\Pr(F_j^*)$, and the corresponding FORM sensitivities $\boldsymbol{\alpha}_j$. These are obtained as a side product of the FORM analysis of $\Pr(F_j^*)$, as the unit vector pointing from the origin to the MLFP,

$$\boldsymbol{\alpha}_j = \frac{\mathbf{u}_j^*}{\|\mathbf{u}_j^*\|}. \tag{30}$$

The probability of the union $\Pr(F_1^* \cup F_2^* \cup \cdots \cup F_i^*)$ is then estimated through [48, 55]

$$\Pr(F_1^* \cup F_2^* \cup \cdots \cup F_i^*) \approx 1 - \Phi_n(\mathbf{b}; \boldsymbol{\rho}). \tag{31}$$

$\Phi_n(\mathbf{b}; \boldsymbol{\rho})$ is the multivariate standard normal CDF with correlation coefficient matrix $\boldsymbol{\rho}$, evaluated at $\mathbf{b}$. The vector $\mathbf{b}$ consists of the i individual FORM reliability indexes $\mathbf{b} = [\beta_1; \ldots; \beta_i]$ associated with the different time intervals. The elements of $\boldsymbol{\rho}$ are the correlation coefficients among the linearized limit state functions of the different time intervals, computed as [48, 55]

$$\rho_{kj} = \boldsymbol{\alpha}_j \boldsymbol{\alpha}_k^\top. \tag{32}$$

wherein $\boldsymbol{\alpha}_j$ and $\boldsymbol{\alpha}_k$ are the row vectors of FORM sensitivities. In evaluating Eq. 32 one must treat $\mathbf{S}_{max,j}$ and $\mathbf{S}_{max,k}$ as two separate random variables.

In the common case that $\mathbf{S}_{max,j}$ and $\mathbf{S}_{max,k}$ are statistically independent of each other, Eq. 32 translates to

$$\begin{aligned}\rho_{jk} =& \alpha_{X_{R,1},j}\,\alpha_{X_{R,1},k} + \cdots + \alpha_{X_{R,n_R},j}\,\alpha_{X_{R,n_R},k} + \\ & \alpha_{S_{\mathrm{ti},1},j}\,\alpha_{S_{\mathrm{ti},1},k} + \cdots + \alpha_{S_{\mathrm{ti},n_{S_{\mathrm{ti}}}},j}\,\alpha_{S_{\mathrm{ti},n_{S_{\mathrm{ti}}}},k}\end{aligned} \tag{33}$$

wherein $\alpha_{X_{R,1},j}$ is the FORM sensitivity associated with the first element of $\mathbf{X}_R$ in time interval j, and $\alpha_{S_{\mathrm{ti},1},j}$ is the one associated with the first element of $\mathbf{S}_{\mathrm{ti}}$ in time interval j.

To illustrate this, consider the case depicted in Figure 2, where each limit state $g(\mathbf{X}_R, \mathbf{S}_{max,j}, \mathbf{S}_{\mathrm{ti}}, t_j)$ consists of two random variables $A = \mathbf{X}_R$ and $S_j = \mathbf{S}_{max,j}$. The corresponding standard normal random variables are U_A and $U_{S,j}$. The correlation among the linearized limit states in time intervals j and k is

$$\rho_{jk} = \alpha_{A,j}\alpha_{A,k}. \tag{34}$$

For the example shown in Figure 2, the resulting correlation coefficients are $\rho_{5,6} = 0.27$, $\rho_{5,7} = 0.30$, and $\rho_{6,7} = 0.34$.

Note that the multivariate standard normal CDF Φ_n in Eq. 31 must be solved numerically. For larger number of dimensions, this evaluation can be challenging [56]. Given that the dimension of Φ_n in Eq. 31 is equal to the number of time intervals considered, which can be high, it is essential that an accurate algorithm for Φ_n is employed. For the numerical investigations in this paper, we utilize the algorithm described in [57].

3.3.2. Sampling-based methods combined with a FORM approximation

When sampling-based methods are used to determine the interval failure probabilities $\Pr(F_i^*)$, we propose to use also the FORM approximation of Eq. 31 to estimate $\Pr[F(t_i)]$. The equivalent FORM reliability indexes in Eq. 31 are determined as

$$\beta_j = \Phi^{-1}\left[\Pr(F_j^*)\right]. \tag{35}$$

Methods for approximating the FORM sensitivities from sampling-based reliability methods have been proposed in the literature [58]. To this end, a linearized limit state function in standard normal space is determined based on samples in or around the failure domain.

In this paper, we use a simpler approach, which is to compute the mean values of all samples in the failure domain $\mathbf{u}_{F,i}^{(k)}$ and normalize the resulting vector:

$$\boldsymbol{\alpha}_j \approx \frac{\sum_k \mathbf{u}_{F,i}^{(k)}}{\|\sum_k \mathbf{u}_{F,i}^{(k)}\|}. \tag{36}$$

We have found that Eq. 36 is sufficiently accurate for most applications with a single design point, and simple to implement.

The approach will fail if multiple design points are present and relevant, i.e. when the failure event within a time interval is itself a series system. In this case, the series system formulation of Eq. 31 must be extended, by considering each linearized limit state associated with a design point as a separate failure event. To identify the multiple design points from failure samples, a clustering algorithm can be run [e.g., 59] and the FORM sensitivities associated with the multiple design points $j = 1, 2, \ldots$ can be approximated by the normalized midpoints of the identified clusters. The component reliability can be approximated by the smallest distance of any sample in the cluster from the origin. If the cross-entropy-based importance sampling approach with Gaussian densities is applied, the different clusters are obtained as a side-product of the structural reliability analysis [46, 47, 60, 61]. Note that if the failure event within one time interval is itself a series system, the computation of the system reliability with Eq. 31 must consider the individual component failure events in all i time intervals jointly.

3.3.3. Computing $\Pr[F(t_i)]$ *through the conditional* $\Pr\left(F_j^*|\mathbf{X}_R = \mathbf{x}_R\right)$

For some structural systems, it is possible to efficiently evaluate the conditional probability of system failure in a time interval j conditional on the condition of the components, $\Pr\left(F_j^*|\mathbf{X}_R = \mathbf{x}_R\right)$. This is of particular interest when the structural system is composed of discrete structural elements, which are modeled as being either in a functioning (= 1) or failed (= 0) state, in function of the deterioration [14]. If the interval failure events are independent for given resistance and deterioration parameters $\mathbf{X}_R = \mathbf{x}_R$, the conditional cumulative probability of failure can be computed as

$$\Pr\left[F\left(t_i\right)|\mathbf{X}_R = \mathbf{x}_R\right] = 1 - \prod_{j=1}^{i}\left[1 - \Pr\left(F_j^*|\mathbf{X}_R = \mathbf{x}_R\right)\right]. \tag{37}$$

If the structure is subject to uncertain permanent loads $\mathbf{S}_{\text{ti}}$, the probability of failure should also be conditioned on those, i.e. $\Pr\left[F\left(t_i\right)|\mathbf{X}_R = \mathbf{x}_R, \mathbf{S}_{\text{ti}} = \mathbf{s}_{\text{ti}}\right]$ should be utilized below and the integrations in Eqs. 38 and 40 should be also over $\mathbf{S}_{\text{ti}}$.

The unconditional cumulative probability of failure is

$$\Pr\left[F\left(t_i\right)\right] = \int_{\Omega_{\mathbf{X}_R}} \Pr\left[F\left(t_i\right)|\mathbf{X}_R = \mathbf{x}_R\right] f_{\mathbf{X}_R}(\mathbf{X}_R)\, d\mathbf{x}_R. \tag{38}$$

All structural reliability methods can be used to compute this (potentially high-dimensional) integral, by defining the equivalent limit state function [14, 62]:

$$g_{F(t_i)}(u_S, \mathbf{x}_R) = u_S - \Phi^{-1}\left\{\Pr\left[F\left(t_i\right)|\mathbf{X}_R = \mathbf{x}_R\right]\right\}, \tag{39}$$

Table 1: Parameters of example 1.

Parameter	Distribution	Mean	Standard deviation
A [mm/yr]	lognormal	0.6	0.5
C [yr]	lognormal	5.0	5.0
w [mm]	deterministic	20	

wherein u_S is a standard normal random variable, and Φ^{-1} is the inverse of the standard normal CDF. The cumulative probability of failure is then

$$\Pr\left[F\left(t_i\right)\right] = \int_{g_{F(t_i)}(u_S, x_R)\leq 0} \varphi(u_S) f_{\mathbf{X}_R}(\mathbf{x}_R)\, d\mathbf{x}_R. \tag{40}$$

which is the classical formulation of a structural reliability problem. φ is the standard normal PDF.

Since FORM can be utilized to approximate the integral in Eq. 40, it is possible to compute the corresponding FORM sensitivities $\boldsymbol{\alpha}_j$. The sensitivity associated with u_S, $\alpha_{U_{S,i}}$, is representative of the influence of the uncertainty in the time-variant load on the reliability.

4. Numerical investigations

We present four examples, to investigate and demonstrate the framework of Section 2 and the methods proposed in Section 3.

The first two examples in Sections 4.1–4.2 are included for illustrative purposes and to facilitate parameter studies. These problems can be solved easily with a variety of methods and exact reference solutions are available. The examples in Sections 4.3–4.4 correspond to the type of applications for which the proposed methods are developed. They include structures whose capacity is a function of the resistances of many elements, all of which are subject to deterioration. Hence the model of $R(t)$ involves a large number of random variables (in the order of 100).

4.1. Example 1: Stochastic deterioration model class (a)

To illustrate stochastic model class (a), we consider a steel plate subject to corrosion. Failure is defined as the corrosion loss exceeding the plate thickness w. The limit state function is

$$g(\mathbf{X}, t) = w - A(t - C). \tag{41}$$

$\mathbf{X} = [A; C]$ are the random variables of the model; A is the corrosion rate and C is the coating life. Corrosion starts only once the coating life is exceeded. The parameters are summarized in Table 1.

Figure 4 shows the limit state functions describing failure at the end of years $1 - 20$ in standard normal space, together with the design points (MLFP). The iterations required in the design point search are also depicted. The modified HLRF algorithm is used [63], with the starting point taken as the MLFP of the subsequent year following Section 3.2.1. It can be observed that only few steps are necessary to find the design point for every year.

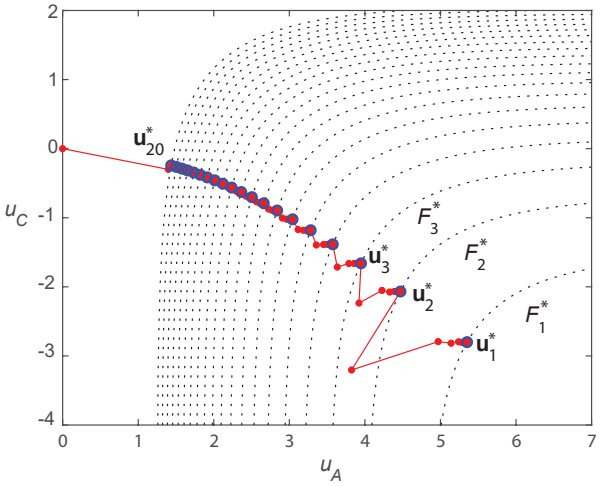

Figure 4: Example 1: Limit state surfaces and MLFPs associated with the failure events at times $t = 1, \ldots, 20$yr in standard normal space. Red dots indicate the steps of the modified HLRF algorithm for finding the MLFPs.

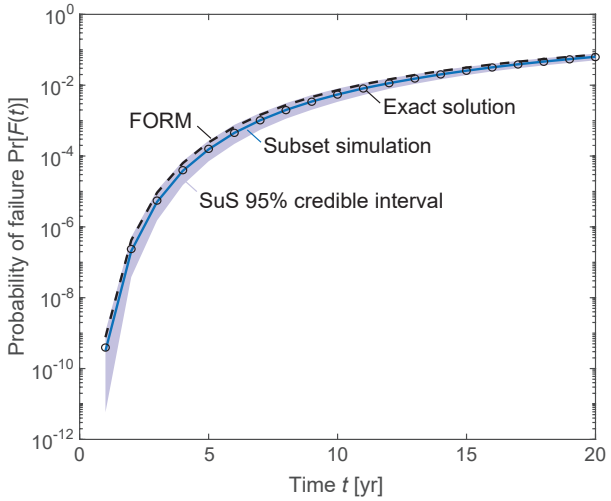

Figure 5: Example 1: The lifetime failure probability computed with FORM and SuS. The latter is shown as the 95% credible interval represented by the colored area, evaluated by 10 repeated runs of SuS.

Additionally, Figure 3 illustrates the sequential SuS solution of this reliability problem. SuS computations are fairly efficient, a total of $16 \cdot 10^3$ limit state function evaluations is sufficient to accurately compute the reliability for all 20 time steps. Nevertheless, FORM would be the method of choice here, since it requires only 813 limit state function evaluations in total.

Figure 5 shows the failure probability $\Pr[F(t)]$ evaluated with FORM and SuS. As expected for this low-dimensional mildly non-linear example, FORM gives fairly accurate results. The mean SuS estimate coincides with the exact solution computed by numerical integration.

4.2. Example 2: Linear Gaussian model

To facilitate numerical investigations of the stochastic deterioration model class (b), we consider an idealized model. The capacity of the system is

$$R(t) = r_0 - At. \tag{42}$$

r_0 is the initial capacity and A is the linear rate of deterioration. Failure occurs when the demand $S(t)$ exceeds $R(t)$, with the failure event described by Eq. 4. The demand is described by its annual maximum $S_{max,j}$, which is iid for all years i. The interval failure probability is evaluated following Eq. 15.

The parameters of the model are summarized in Table 2. They are motivated by the example of a pressurized steel pipe subject to corrosion[13]. All random variables are modeled by normal distributions to enable an analytical solution.

[13]In a steel pipe, the pressure resistance $R(t)$ of the pipe is as proportional to $2S_y \frac{d-d_{UC}(t)}{D_p}$, with S_y the yield stress, D_p the diameter of the pipe, d the wall thickness of the pipe and $d_{UC}(t)$ the general corrosion depth [64, 65]. By ignoring localized corrosion effects and assuming d_{UC} to be a linear function of time, the expression of $R(t)$ in Eq. 42 is obtained.

Table 2: Parameters of example 2.

Parameter	Distribution	Mean	Standard deviation
A [MPa/yr]	normal	0.2	0.2
$S_{max,j}$ [MPa]	normal	40	σ_S
r_0 [MPa]	deterministic	r_0	
$\epsilon_m[MPa]$	normal	0	0.5

The standard deviation of the demand σ_S is varied, to examine the effect of different ratios between the uncertainty in R and the uncertainty in S_{max_j}. It is

$$\sigma_S = ratio \times \mu_S \frac{\sigma_A \, 20\text{yr}}{r_0 - \mu_A \, 20\text{yr}}. \tag{43}$$

ratio is the ratio between the c.o.v. of S_{max_j} and the c.o.v. of R at year 20.

r_0 is selected such that probability of failure in one year without deterioration is 10^{-6}:

$$\Phi\left(-\frac{r_0 - \mu_S}{\sigma_S}\right) = 10^{-6} \quad \Longleftrightarrow \quad r_0 = -\Phi^{-1}(10^{-6})\sigma_S + \mu_S. \tag{44}$$

Since the limit state function is linear and all random variables are normal, a FORM analysis gives the exact result (bare the approximation made by the time discretization). Figure 6 presents the resulting probabilities of the interval failure event $\Pr(F_i^*)$ for years $i = 1, \ldots, 20$.

Figure 7 presents the FORM sensitivity $\alpha_{A,j}$ of the deterioration parameter A in function of time interval j for different *ratio*s. Note that, since in each year there are only two random variables active, it is $\alpha_{S_{max,j}} = \sqrt{1 - \alpha_{A,j}^2}$. Furthermore, since all $S_{max,j}$ are iid, the correlation coefficient among the interval failure limit state functions in two years j and k is given by Eq. 34 as $\rho_{jk} = \alpha_{A,j}\alpha_{A,k}$.

Figure 8 shows the reliability in function of time computed with the (here exact) FORM formulation of Eq. 31.

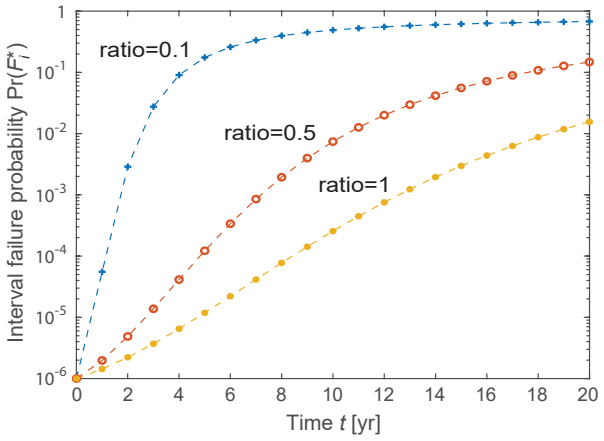

Figure 6: Example 2: Interval failure probabilities for years $i = 1, \ldots, 20$ for different uncertainty ratios.

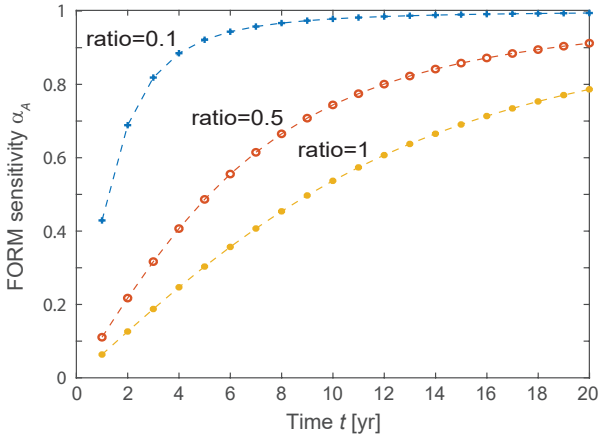

Figure 7: Example 2: FORM sensitivity of deterioration model parameter A.

The bounds following Eq. 20 are provided additionally. For $ratio = 1$, the uncertainty in the load process dominates, and the assumption of independence among failure events in different years (the upper bound of Eq. 20) is a reasonable one. Conversely, for $ratio = 0.1$, the uncertainty in the deterioration process dominates, hence the cumulative $\Pr[F(t)]$ is closer to the lower bound. In other words, the larger the $\alpha_{A,i}$, and hence the correlation coefficients among the interval failure event limit state functions, the closer $\Pr[F(t)]$ will be to the lower bound.

4.2.1. Conditional on inspection results

We additionally consider two inspection results and compute the updated probability of failure, following Section 2.4. Inspections are performed at times $\mathbf{t}_Z = [10; 15]$yr and result in measurements of the remaining pressure capacity, $\mathbf{m} = [47.04; 46.84]$MPa.

The measurements are imperfect and are related to the true capacity by

$$m_j = R(t_{Z,j}) + \epsilon_j, \tag{45}$$

with ϵ_j being a normal distributed measurement error with zero mean and standard deviation $\sigma_\epsilon = 0.5$MPa.

With this model, an analytical solution for the posterior probability distribution of A given the measurement result m_j is available. It is the normal distribution with updated mean and standard deviation:

$$\mu''_A = \mu_A + \rho_{A,M}\,\sigma_A \frac{m_j - (r_0 - \mu_A t_{Z,j})}{\sqrt{\sigma_A^2 t_{Z,j}^2 + \sigma_\epsilon^2}}, \tag{46}$$

$$\sigma''_A = \sigma_A \sqrt{1 - \rho_{A,M}^2}. \tag{47}$$

wherein μ_A and σ_A are the prior mean and standard deviation of A and $\rho_{A,M}$ is the correlation coefficient between A and the measurement outcome:

$$\rho_{A,M} = -\frac{\sigma_A t_{Z,j}}{\sqrt{\sigma_A^2 t_{Z,j}^2 + \sigma_\epsilon^2}}. \tag{48}$$

To consider two measurements, Eqs. 46 and 47 can be applied twice, whereby the posterior moments conditional on the first measurement are taken as prior moments with the second measurement.

Since also the posterior of A is normal distributed, all posterior results can be computed exactly with a FORM analysis, in which the prior distribution of A is replaced by the posterior distributions.

Figure 9 shows the posterior interval failure probabilities $\Pr\left[F_j^* | Z(t_Z)\right]$ for $ratio = 0.5$, conditional on the first measurement and conditional on both measurements. As discussed in Section 2.4, all interval failure probabilities need to be computed from the first time interval on.

Figure 10 shows the corresponding FORM sensitivities of deterioration parameter A. The contribution of A to the failure probability reduces because the uncertainty in A is reduced by each inspection result. Note that this conclusion would also hold for less favorable inspection results, because the reduction in the uncertainty of A is independent of the measured value, Eq. 47.

Figure 11 shows the posterior cumulative probability of failure $\Pr[F(t_i)|Z(t_i)]$, Eq. 21. The dashed lines are included to emphasize that in computing $\Pr[F(t_i)|Z(t_i)]$, the entire history leading up to t_i has to be conditioned on $Z(t_i)$, following Section 2.4.

Figure 12 shows the associated bounds. It highlights that with increasing amount of information, $\Pr[F(t_i)|Z(t_i)]$ approaches the upper bound, which is a direct consequence of the decreased importance of A, Figure 10.

Finally, Figure 13 exhibits the hazard function of the inspected structure. It is computed by utilizing the $\Pr[F(t_i)|Z(t_Z)]$ of Figure 11 as an input to Eqs. 8–10, as described in Section 2.4.

4.3. Example 3: Ship cross-section subject to corrosion

A cross-section of a ship structure is considered (Figure 14). The steel frame is subject to spatially distributed corrosion, which is modeled by a hierarchical model combined

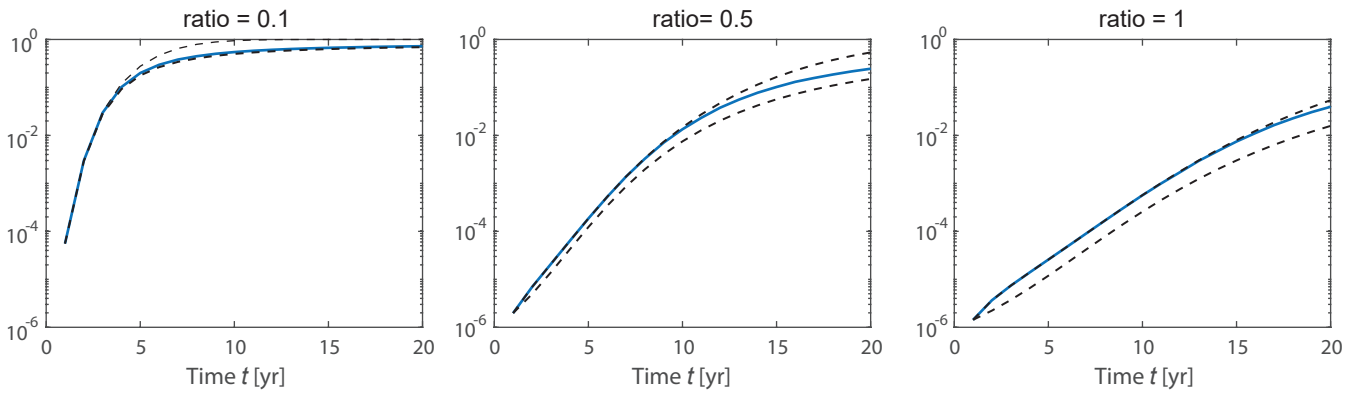

Figure 8: Example 2: Cumulative failure probability computed with the FORM approach, together with the bounds following Eq. 20.

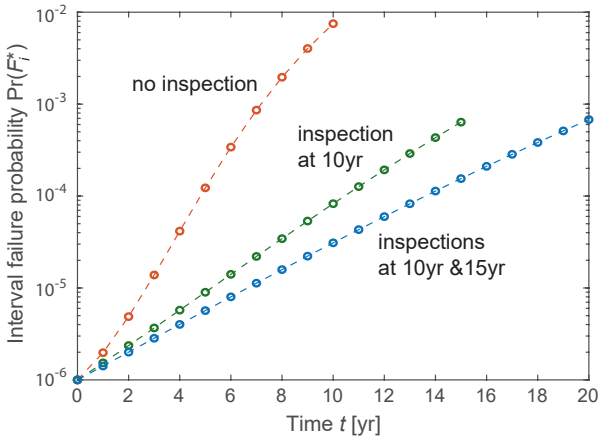

Figure 9: Example 2: Interval failure probabilities for years $i = 1, \ldots, 20$ conditional on the inspection results. Results shown for $ratio = 0.5$.

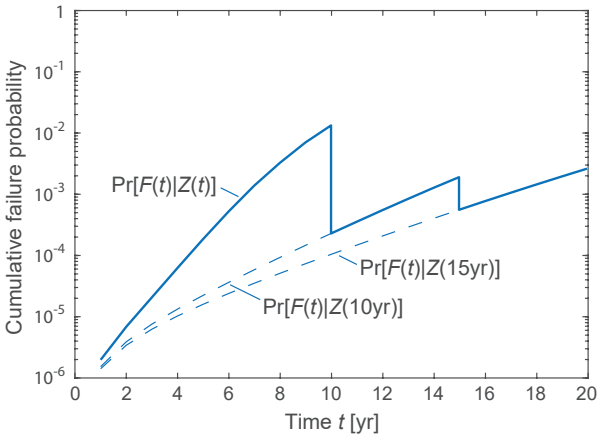

Figure 11: Example 2: Cumulative failure probability conditional on the inspection result for $ratio = 0.5$. The through line shows the probability at time t conditional on all information available up to time t (filtering). The dashed lines represent the probability conditional on a fixed set of measurements (smoothing).

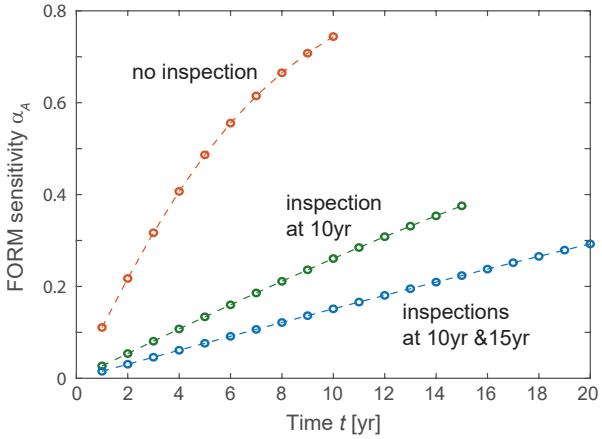

Figure 10: Example 2: FORM sensitivity of deterioration model parameter A, conditional on inspection results. Results shown for $ratio = 0.5$.

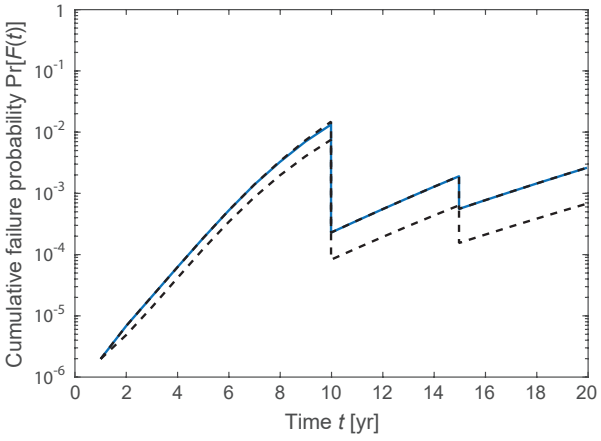

Figure 12: Example 2: Cumulative failure probability conditional on the inspection result for $ratio = 0.5$, together with bounds.

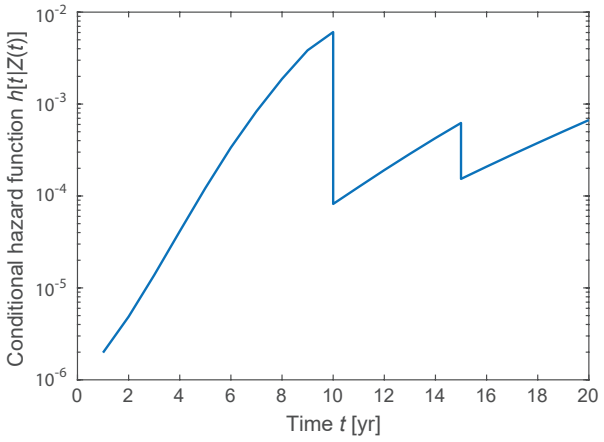

Figure 13: Example 2: Hazard function conditional on the inspection result.

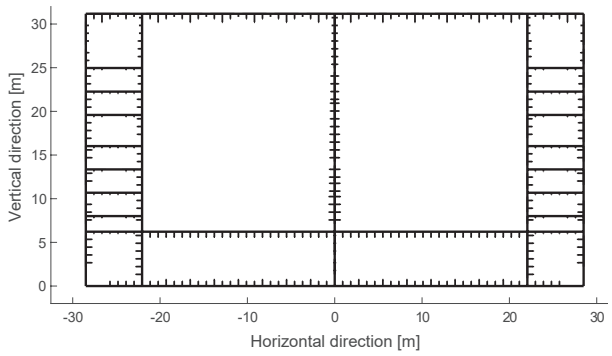

Figure 14: Example 3: Cross-section of the ship structure [66].

with a random field (RF) model. The RF is represented by spectral decomposition.

The frame is subject to bending caused by stillwater and wave loading. The corresponding limit state function is

$$g\left(\mathbf{X}_R, \mathbf{X}_S, \mathbf{S}_{max,j}, t_j\right) = X_m M_R(\mathbf{X}_d, t_i) - X_{sw} M_{sw,j} - X_{wv} M_{wv,j}, \tag{49}$$

wherein M_R is the moment capacity, which is a function of deterioration parameters $\mathbf{X}_d$ and subject to structural model uncertainty X_m. $M_{sw,j}$ is the stillwater bending moment, which is affected by self-weight, cargo and ballast, and X_{sw} is the associated model uncertainty; $M_{wv,j}$ is the bending moment caused by wave loading and X_{wv} is the associated model uncertainty. It is $\mathbf{X}_R = [\mathbf{X}_d; X_m]$, $\mathbf{X}_S = [X_{sw}; X_{wv}]$ and $\mathbf{S}_{max,j} = [M_{sw,j}; M_{wv,j}]$.

$M_{wv,j}$ is associated with the annual maximum wave load, whereas $M_{sw,j}$ is representative of the random-point-in-time stillwater moment. The stillwater moment is constant during a single voyage of the ship. Hence if the time interval duration is selected as that of a ship voyage (in the order of weeks to a month), this limit state is exact. If longer time intervals are used in the analysis, this limit state represents a (possibly non-conservative) approximation. However, the approximation error is expected to be

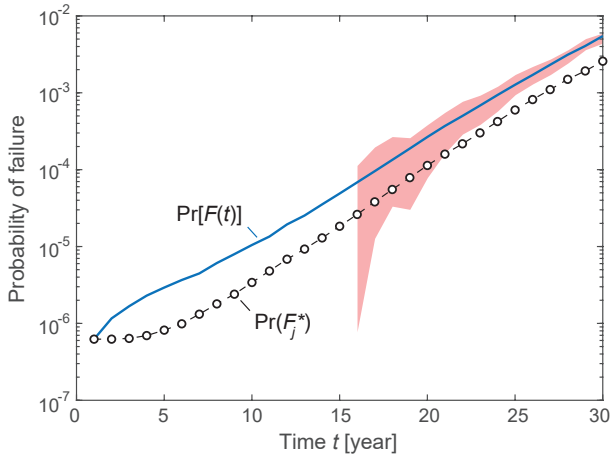

Figure 15: Example 3: Interval failure probability $\Pr(F_j^*)$ and cumulative failure probability $\Pr[F(t)]$ of the ship steel frame, computed with the proposed SuS-FORM algorithm. The 95% credible interval of a direct MCS solution of $\Pr[F(t)]$ from $n_s = 25 \cdot 10^3$ samples is provided for comparison (in red).

limited, since the cargo in subsequent voyages is likely to be correlated (with higher correlation at lag 2 than at lag 1). Therefore, modeling M_{sw} as constant within one year and independent among years is a reasonable model. Alternatively, this modeling choice can be justified through the use of Turkstra's rule, because the wave-induced moment is dominating the reliability (over the stillwater moment) [67, 68].

The complete model and parameters are described in [66]. In total, the problem includes 106 random variables.

The reliability is evaluated in one-year time intervals with SuS, utilizing 10^3 samples at each intermediate subset. The sequential approach of Section 3.2.2 is employed to compute the interval failure probabilities for years $j = 1, \ldots, 30$, resulting in a total of around $17 \cdot 10^3$ limit state function evaluations. Based on $\Pr(F_j^*)$, the failure probability $\Pr[F(t)]$ is evaluated with the FORM system approximation following Section 3.3.2. The results are shown in Figure 15. Note that the MCS solution provided for verification requires $750 \cdot 10^3$ limit state function evaluations, corresponding to 30 [years] times $25 \cdot 10^3$ samples.

Additionally, Figure 16 shows the hazard function $h(t)$ evaluated from $\Pr[F(t)]$ according to Eq. 10. Note that $h(t)$ is lower than the interval failure probability (as is $f_T(t)$, Eq. 8).

4.4. Example 4: Steel frame subject to fatigue

We consider a steel frame subject to fatigue deterioration at selected joints (the hot spots), Figure 17. Details of this example are provided in [14], where the interval failure probability was computed, but not the cumulative $\Pr[F(t)]$.

The evolution of the system resistance is described by employing a fatigue crack growth model at each hot spot. The uncertain parameters of the model at each hot spot are:

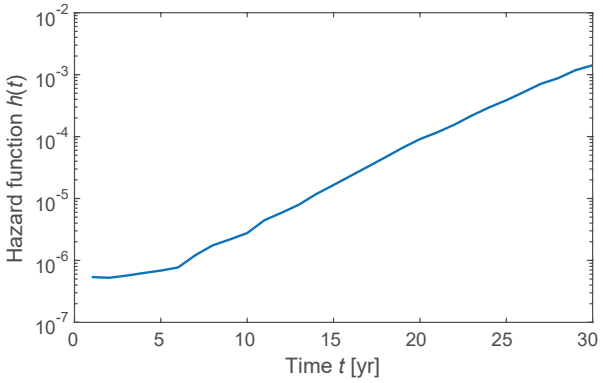

Figure 16: Example 3: Hazard function of the ship section.

- initial fatigue crack depth D_0,
- material parameter C,
- scale parameter K of the hot spot stress distribution
- model uncertainties $B_{\Delta S}$ and B_{SIF}

This leads to a total of 110 random variables $\mathbf{X}_R$ describing the evolution of the structural capacity.

The structure is subject to a time-varying horizontal load, modeled by its annual maximum $S_{max,j}$. The structural reliability is evaluated by computing the probability of failure in function of the hot spot conditions, which implicitly results in the conditional $\Pr[F_j^*|\mathbf{X}_R = \mathbf{x}_R]$.

The probability of failure of the Zayas frame is computed following Section 3.3.3 and SuS is employed to evaluate the reliability following Eq. 40. SuS is run with 1000 MCMC samples per subset level and a conditional probability of each intermediate event of 0.1. Results are shown in Figure 18. The statistics of $\Pr[F(t_i)]$ are determined from 500 independent simulation runs.

Figure 19 additionally shows the bounds on the failure probability following Eq. 20. In the first few years, when deterioration is still negligible, $\Pr[F(t)]$ is close to the upper bound. Thereafter, it approaches the lower bound, indicating that the uncertainty on the condition of the structure, i.e. on $R(\mathbf{X}_R, t)$, dominates the reliability.

4.4.1. With inspection results

Additionally, we include results from inspections on the hot spots. Inspections are performed every 10 years, with 6 varying hot spots checked at each inspection, with the exception of year 40, when only 4 hot spots are inspected. For simplicity it is assumed that no fatigue cracks are detected at any of the inspections.

Figure 20 shows the probability of failure of the structure conditional on the inspection outcomes. At each time t, $\Pr[F(t)|Z(t)]$ is conditioned on inspection results up to time t. The computation of $\Pr[F(t)|Z(t)]$ is performed according to Section 2.4 and as illustrated in more details in Section 4.2.1.

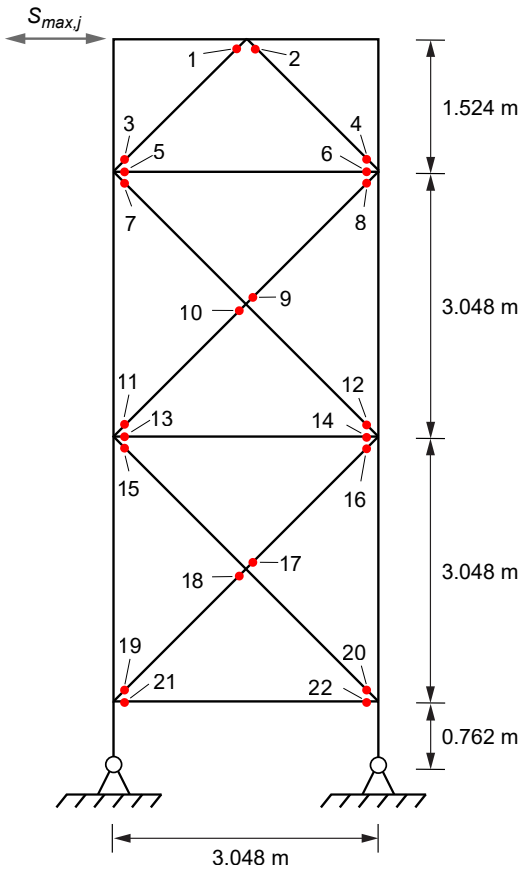

Figure 17: Example 4: Steel frame loaded with $S_{max,j}$. Red dots indicate the fatigue hot spots.

5. Concluding remarks

The reliability analysis of deteriorating structural systems requires efficient computational procedures, because the reliability needs to be evaluated at multiple points in time. When computing the reliability conditional on inspection or monitoring data, the analysis must be repeated for the entire period every time new information is available, as discussed in Section 2.4. The situation is even more severe when performing risk-based planning of inspection and monitoring, since all computations need to be repeated many times for different potential inspection or monitoring outcomes [69]. All this motivates the development of efficient approaches to compute the time-variant reliability of deteriorating structures. In this paper, we follow the strategy of discretizing time and representing the time-variant reliability problem by a series of time-invariant reliability problems.

As demonstrated in this paper, smart sequential computation of the time-invariant reliability at different times t can reduce the number of limit state function evaluations by a factor in the order of 10, which is substantial. Importantly, we presented a simple way of computing the cumulative probability of failure $\Pr[F(t)]$ based on advanced sampling methods without additional limit state function

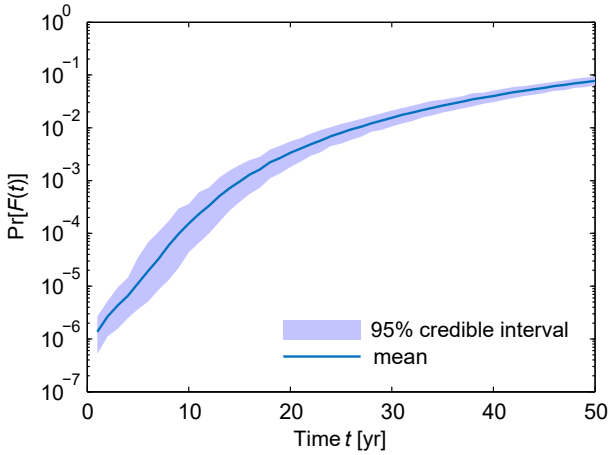

Figure 18: Example 4: Failure probability $\Pr[F(t)]$ of the steel frame.

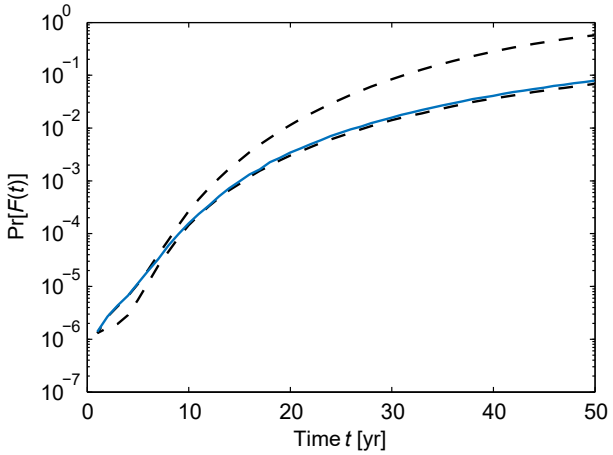

Figure 19: Example 4: Bounds on the failure probability $\Pr[F(t)]$ of the steel frame, together with the best estimate.

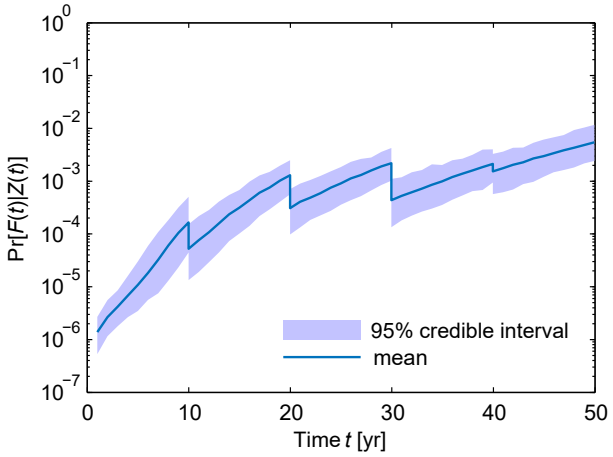

Figure 20: Example 4: Failure probability of the steel frame conditional on inspection results.

evaluations, which can further reduce compuational cost by a factor of 10 or more. For example, the complete lifetime reliability of the ship structure in Section 4.3 was evaluated accurately with $17 \cdot 10^3$ limit state function evaluations. For a similarly accurate crude Monte Carlo simulation, which has been used frequently in the literature, in the order of 10^7 limit state function evaluations would be necessary.

The proposed procedure involves approximations at multiple steps. Firstly, the definition of the interval failure probability following Eqs. 15 or 17 is not exact. As long as the problem involves only one time-variant load variable and the time intervals are selected sufficiently small, the error is small, bounded and always conservative. If multiple time-variant load processes are present, the quality of the approximation depends on how well these can be approximated by time-invariant random variables, e.g. through Turkstra's rule. In many, possibly most practical cases, such an approximation is sufficiently good, albeit not generally conservative [e.g., 32]. Importantly, this approximation error can be evaluated without considering deterioration. Secondly, an error is introduced in computing the interval failure probabilities with FORM/SORM or sampling-based methods. This approximation error is discussed in the general literature on structural reliability methods and hence is well-understood. Thirdly, the FORM-based approximation of the series system evaluation introduces another error. In all investigated cases, we found this error to be so small that it could not be quantified relative to a Monte Carlo reference solution. Furthermore, this error is bounded by the bounds of Eq. 20.

As we emphasized, special care is needed when considering results from inspection and monitoring. The literature on Bayesian updating of the reliability and on reliability- and risk-based planning of inspections and monitoring has not always rigorously defined and computed the exact time-variant reliability of structural systems. (For structural components, the limit state functions are mostly of the first class, Section 2.2, and therefore the equivalence between the point-in-time-failure and the cumulative failure event holds, which avoids the problem.) In particular, the fact that the conditional reliability must be computed by considering all interval failure events from time 0 on seems not to have been recognized previously.

We have not considered methods that directly solve the outcrossing problem. We are of the opinion that as long as the interval failure probability can be defined by Eqs. 15 or 17, it is at present preferable to follow the approach outlined in this paper. General solutions to the outcrossing problem, insofar as they are not restricted to some special cases, are conceptually and computationally demanding and introduce approximation errors of their own. Nevertheless, in light of new developments in efficient methods for structural reliability analysis, we believe that it is worthwhile to revisit algorithms for solving the general outcrossing problem.

6. Acknowledgments

This work was supported by the Deutsche Forschungsgemeinschaft (DFG) through Grant STR 1140/3-2.

References

[1] H. O. Madsen, S. Krenk, N. C. Lind, Methods of Structural Safety, Dover Publications, 1986.
[2] R. E. Melchers, Structural reliability analysis and prediction, John Wiley, 1999.
[3] B. R. Ellingwood, Risk-informed condition assessment of civil infrastructure: state of practice and research issues, Structure and Infrastructure Engineering 1 (1) (2005) 7–18.
[4] R. Rackwitz, Computational techniques in stationary and non-stationary load combination - A review and some extensions, Journal of Structural Engineering (Madras) 25 (1) (1998) 1–20.
[5] Y. Mori, B. R. Ellingwood, Reliability-based service life assessment of aging concrete structures, Journal of Structural Engineering, Trans. ASCE 119 (5) (1993) 1600–1621.
[6] A. Lentz, G. Defaux, R. Rackwitz, Principles of Reliability Calculations for Deteriorating Structures, in: Life-Cycle Performance of Deteriorating Structures, American Society of Civil Engineers, Reston, VA, 2003, pp. 92–101.
[7] C. Andrieu-Renaud, B. Sudret, M. Lemaire, The PHI2 method: a way to compute time-variant reliability, Reliability Engineering & System Safety 84 (1) (2004) 75–86.
[8] G. Schall, M. H. Faber, R. Rackwitz, The Ergodicity Assumption for Sea States in the Reliability Estimation of Offshore Structures, Journal of Offshore Mechanics and Arctic Engineering 113 (3) (1991) 241.
[9] J. M. van Noortwijk, J. A. van der Weide, M.-J. Kallen, M. D. Pandey, Gamma processes and peaks-over-threshold distributions for time-dependent reliability, Reliability Engineering & System Safety 92 (12) (2007) 1651–1658.
[10] D. V. Val, R. E. Melchers, Reliability of deteriorating RC slab bridges, Journal of Structural Engineering, Trans. ASCE 123 (12) (1997) 1638–1644.
[11] D. V. Val, M. G. Stewart, R. E. Melchers, Life-cycle performance of RC bridges: probabilistic approach, Computer-Aided Civil and Infrastructure Engineering 15 (1) (2000) 14–25.
[12] M. G. Stewart, A. Al-Harthy, Pitting corrosion and structural reliability of corroding RC structures: Experimental data and probabilistic analysis, Reliability Engineering and System Safety 93 (2008) 373–382.
[13] A. Zayed, Y. Garbatov, C. G. Soares, Reliability of ship hulls subjected to corrosion and maintenance, Structural Safety 43 (2013) 1–11.
[14] R. Schneider, S. Thöns, D. Straub, Reliability analysis and updating of deteriorating systems with subset simulation, Structural Safety 64 (2017) 20–36.
[15] H. S. Sousa, J. D. Sørensen, P. H. Kirkegaard, J. M. Branco, P. B. Lourenço, On the use of ndt data for reliability-based assessment of existing timber structures, Engineering Structures 56 (2013) 298–311.
[16] S. A. Faroz, N. N. Pujari, S. Ghosh, Reliability of a corroded rc beam based on bayesian updating of the corrosion model, Engineering Structures 126 (2016) 457–468.
[17] Ditlevsen O., H. O. Madsen, Structural Reliability Methods, John Wiley & Sons, 1996.
[18] A. C. Estes, D. M. Frangopol, Repair Optimization of Highway Bridges Using System Reliability Approach, Journal of Structural Engineering 125 (7) (1999) 766–775.
[19] V. Sarveswaran, M. B. Roberts, Reliability analysis of deteriorating structures the experience and needs of practising engineers, Structural Safety 21 (4) (1999) 357–372.
[20] G. Barone, D. M. Frangopol, Reliability, risk and lifetime distributions as performance indicators for life-cycle maintenance of deteriorating structures, Reliability Engineering & System Safety 123 (2014) 21–37.
[21] M. Rausand, A. Høyland, System Reliability Theory: Models, Statistical Methods, and Applications, Wiley, 2004.
[22] J. Schneider, T. Vrouwenvelder, Introduction to Safety and Reliability of Structures, IABSE, Zürich, 2017.
[23] R. Rackwitz, Optimizationthe basis of code-making and reliability verification, Structural safety 22 (1) (2000) 27–60.
[24] M. D. Pandey, J. Van Der Weide, Stochastic renewal process models for estimation of damage cost over the life-cycle of a structure, Structural Safety 67 (2017) 27–38.
[25] R. Rackwitz, Optimizing systematically renewed structures, Reliability Engineering & System Safety 73 (3) (2001) 269–279.
[26] H. Streicher, R. Rackwitz, Time-variant reliability-oriented structural optimization and a renewal model for life-cycle costing, Probabilistic Engineering Mechanics 19 (1-2) (2004) 171–183.
[27] M. Chryssanthopoulos, T. Righiniotis, Fatigue reliability of welded steel structures, Journal of Constructional Steel Research 62 (11) (2006) 1199–1209.
[28] M. Abdel-Hameed, A gamma wear process, IEEE Transactions on Reliability 24 (2) (1975) 152–153.
[29] J. Van Noortwijk, A survey of the application of gamma processes in maintenance, Reliability Engineering & System Safety 94 (1) (2009) 2–21.
[30] R. Rackwitz, B. Fiessler, Structural reliability under combined random load sequences, Computers & Structures 9 (5) (1978) 489–494.
[31] C. J. Turkstra, H. O. Madsen, Load Combinations in Codified Structural Design, Journal of the Structural Division, Trans. ASCE 106 (12) (1980) 2527–2543.
[32] H. O. Madsen, L. Tvedt, Methods for time-dependent reliability and sensitivity analysis, Journal of Engineering Mechanics 116 (10) (1990) 2118–2135.
[33] O. Ditlevsen, Narrow Reliability Bounds for Structural Systems, Journal of Structural Mechanics 7 (4) (1979) 453–472.
[34] D. V. Val, M. G. Stewart, R. E. Melchers, Life-Cycle Performance of RC Bridges: Probabilistic Approach, Computer-Aided Civil and Infrastructure Engineering 15 (2000) 14–25.
[35] H. O. Madsen, Model updating in reliability theory, in: ICASP 5, Vancouver, Canada., 1987, pp. 564–577.
[36] R. Sindel, R. Rackwitz, Problems and Solution Strategies in Reliability Updating, Journal of Offshore Mechanics and Arctic Engineering 120 (2) (1998) 109.
[37] D. Straub, Reliability updating with equality information, Probabilistic Engineering Mechanics 26 (2011) 254–258.
[38] D. Straub, I. Papaioannou, Bayesian updating with structural reliability methods, Journal of Engineering Mechanics 141 (3) (2015) 04014134.
[39] D. Straub, I. Papaioannou, W. Betz, Bayesian analysis of rare events, Journal of Computational Physics 314 (2016) 538–556.
[40] D. Straub, Stochastic modeling of deterioration processes through dynamic Bayesian networks, Journal of Engineering Mechanics 135 (10) (2009) 1089–1099.
[41] J. Ching, Y.-C. Chen, Transitional markov chain monte carlo method for bayesian model updating, model class selection, and model averaging, Journal of engineering mechanics 133 (7) (2007) 816–832.
[42] I. Papaioannou, C. Papadimitriou, D. Straub, Sequential importance sampling for structural reliability analysis, Structural Safety 62 (2016) 66–75.
[43] M. Hohenbichler, R. Rackwitz, Improvement Of Second-Order Reliability Estimates by Importance Sampling, Journal of Engineering Mechanics 114 (12) (1988) 2195–2199.
[44] R. Rackwitz, Reliability analysis – A review and some perspectives, Structural Safety 23 (4) (2001) 365–395.
[45] P. Koutsourelakis, H. Pradlwarter, G. Schuëller, Reliability of structures in high dimensions, part I: algorithms and applications, Probabilistic Engineering Mechanics 19 (4) (2004) 409–417.
[46] N. Kurtz, J. Song, Cross-entropy-based adaptive importance sampling using Gaussian mixture, Structural Safety 42 (2013) 35–44.

[47] I. Papaioannou, S. Geyer, D. Straub, Improved cross entropy-based importance sampling with a flexible mixture model, Reliability Engineering & System Safety 191 (2019) 106564. doi:https://doi.org/10.1016/j.ress.2019.106564.
[48] M. Hohenbichler, R. Rackwitz, Non-Normal Dependent Vectors in Structural Safety, Journal of the Engineering Mechanics Division 107 (6) (1981) 1227–1238.
[49] A. Der Kiureghian, P. Liu, Structural Reliability under Incomplete Probability Information, Journal of Engineering Mechanics 112 (1) (1986) 85–104.
[50] S. K. Au, J. L. Beck, Estimation of small failure probabilities in high dimensions by subset simulation, Probabilistic Engineering Mechanics 16 (4) (2001) 263–277.
[51] I. Papaioannou, W. Betz, K. Zwirglmaier, D. Straub, MCMC algorithms for Subset Simulation, Probabilistic Engineering Mechanics 41 (2015) 89–103.
[52] R. Y. Rubinstein, D. P. Kroese, Simulation and the Monte Carlo method, Vol. 10, John Wiley & Sons, 2016.
[53] K. Breitung, On subsets and onions: Lost in outer space.
[54] H.-J. Kim, D. Straub, Sequential algorithms for lifetime reliability analysis of structures subject to deterioration, in: Proc. ICASP13, Seoul, Korea, 2019.
[55] A. Der Kiureghian, First- and second-order reliability methods. Chapter 14, in Engineering design reliability handbook, edited by E. Nikolaidis et al., CRC Press, Boca Raton, FL, 2005.
[56] A. Genz, F. Bretz, Computation of multivariate normal and t probabilities, Springer, 2009.
[57] Z. I. Botev, The normal law under linear restrictions: simulation and estimation via minimax tilting, Journal of the Royal Statistical Society: Series B (Statistical Methodology) 79 (1) (2017) 125–148.
[58] R. E. Melchers, M. Ahammed, A fast approximate method for parameter sensitivity estimation in Monte Carlo structural reliability, Computers and Structures 82 (2004) 55–61.
[59] M. Ester, H.-P. Kriegel, J. Sander, X. Xu, A Density-Based Algorithm for Discovering Clusters in Large Spatial Databases with Noise, in: Second international conference on knowledge discovery and data mining, AAAI Press, 1996, pp. 226–231.
[60] T. Kim, J. Song, Generalized Reliability Importance Measure (GRIM) using Gaussian mixture, Reliability Engineering & System Safety 173 (2018) 105–115.
[61] S. Geyer, I. Papaioannou, D. Straub, Cross entropy-based importance sampling using Gaussian densities revisited, Structural Safety 76 (2019) 15–27.
[62] Y. Wen, H.-C. Chen, On fast integration for time variant structural reliability, Probabilistic Engineering Mechanics 2 (3) (1987) 156–162.
[63] P.-L. Liu, A. Der Kiureghian, Optimization algorithms for structural reliability, Structural Safety 9 (3) (1991) 161–177.
[64] M. Ahammed, R. Melchers, Reliability estimation of pressurised pipelines subject to localised corrosion defects, International Journal of Pressure Vessels and Piping 69 (3) (1996) 267–272.
[65] D. Straub, Generic Approaches to Risk Based Inspection Planning for Steel Structures, Phd, ETH Zürich (2004).
[66] H. Kim, D. Straub, Reliability analysis and updating of inspected ship structures subject to spatially variable corrosion, in: 12th International Conference on Structural Safety & Reliability (ICOSSAR 2017), Vienna, Austria, 2017.
[67] B. Gaspar, C. G. Soares, Hull girder reliability using a monte carlo based simulation method, Probabilistic Engineering Mechanics 31 (2013) 65 – 75.
[68] A. P. Teixeira, C. Guedes Soares, N.-Z. Chen, G. Wang, Uncertainty analysis of load combination factors for global longitudinal bending moments of double-hull tankers, Journal of Ship Research 57 (1) (2013) 42–58.
[69] J. Luque, D. Straub, Risk-based optimal inspection strategies for structural systems using dynamic Bayesian networks, Structural Safety 76 (2019) 68–80.